Journal of Medicinal Chemistry

Article

pubs.acs.org/jmc

The Antitumor Agent PBT-1 Directly Targets HSP90 and hnRNP A2/B1 and Inhibits Lung Adenocarcinoma Growth and Metastasis

Chi-Yuan Chen,[†,‡,§,∞] Shuenn-Chen Yang,[∥,∞] Kuo-Hsiung Lee,[⊥,#] Xiaoming Yang,[#] Lin-Yi Wei,[#] Lu-Ping Chow,[∇,○] Tzu-Chien V. Wang,[◆] Tse-Ming Hong,[¶] Jau-Chen Lin,[+] Crysline Kuan,[×] and Pan-Chyr Yang*[,∥,◇,△]

[†]Research Center for Industry of Human Ecology, [‡]Graduate Institute of Health Industry Technology, and [§]Department of Nutrition and Health Sciences, Chang Gung University of Science and Technology, Kwei-San, Tao-Yuan, Taiwan

[∥]Institute of Biomedical Sciences, Academia Sinica, Taipei, Taiwan

[⊥]Chinese Medicine Research and Development Center, China Medical University and Hospital, Taichung, Taiwan

[#]Natural Products Research Laboratories, UNC Eshelman School of Pharmacy, University of North Carolina, Chapel Hill, North Carolina 27599, United States

[∇]Graduate Institute of Biochemistry and Molecular Biology, College of Medicine, National Taiwan University, Taipei, Taiwan

[○]Department of Medical Genetics, National Taiwan University Hospital, Taipei, Taiwan

[◆]Department of Molecular and Cellular Biology, School of Medicine, Chang Gung University, Kwei-San, Tao-Yuan, Taiwan

[¶]Institute of Clinical Medicine, National Cheng Kung University, Tainan, Taiwan

[+]Department of Respiratory Therapy, Fu-Jen Catholic University, New Taipei, Taiwan

[×]Department of Microbiology, University of Washington, Seattle, Washington 98195, United States

[◇]NTU Center of Genomic Medicine and [△]Department of Internal Medicine, College of Medicine, National Taiwan University, Taipei, Taiwan

Supporting Information

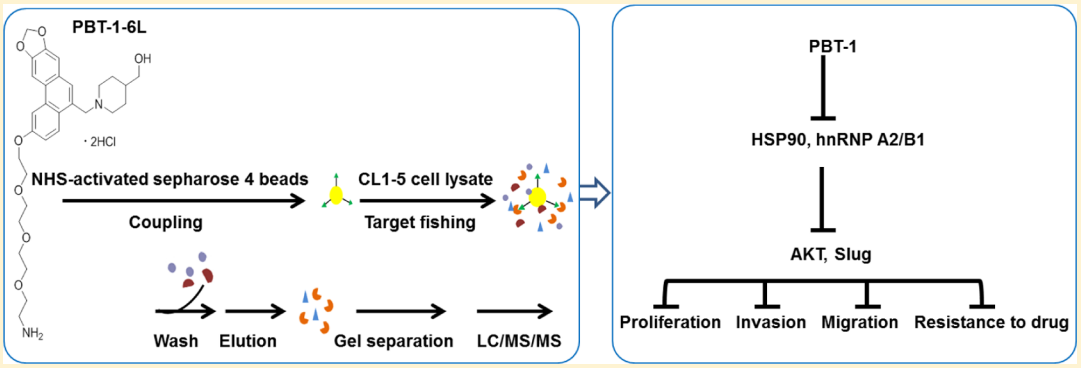

ABSTRACT: Natural products are the major sources of currently available anticancer drugs. We recently reported that phenanthrene-based tylophorine derivative-1 (PBT-1) may be a potential antitumor agent for lung adenocarcinoma. We therefore examined the direct targets of PBT-1 and their effects in inhibiting lung adenocarcinoma. We found that PBT-1 reduced the level of Slug and inhibits the migration, invasion, and filopodia formation of lung adenocarcinoma CL1-5 cells in vitro. In addition, PBT-1 displayed in vivo antitumor and antimetastasis activities against subcutaneous and orthotopic xenografts of CL1-5 cells in nude mice. Chemical proteomics showed that heat shock protein 90 (HSP90) and heterogeneous nuclear ribonucleoproteins A2/B1 (hnRNP A2/B1) bound PBT-1 in CL1-5 cells. Inhibition of HSP90 and hnRNP A2/B1 reduced the activation of AKT and Slug expression. Taken together, these findings suggest that PBT-1 binds to HSP90 and/or hnRNP A2/B1 and initiates antitumor activities by affecting Slug- and AKT-mediated metastasis and tumorigenesis.

INTRODUCTION

Lung cancer is the most common cause of cancer death worldwide, and lung adenocarcinoma is the major dominant cell type.[1] Although surgery remains the treatment of choice in patients with early-stage lung cancer, 40% of these patients may relapse within 5 years.[2] Moreover, widespread metastasis at diagnosis frequently precludes surgery.[2] Therefore, the development of

Received: August 9, 2013
Published: January 15, 2014

   dx.doi.org/10.1021/jm401686b | J. Med. Chem. 2014, 57, 677−685

compounds with pharmacologic properties and antitumor activities in lung adenocarcinoma patients at high risk of recurrence or metastasis may help improve their management.

Natural products have been the major source of currently available anticancer drugs. Tylophorine belongs to a group of natural plant compounds, the phenanthroindolizidine alkaloids, which have high potency against various cancer cell lines.[3−5] However, trials of tylocrebrine, a positional isomer of tylophorine, had to be discontinued because of adverse effects on the central nervous system (CNS).[6] Molecular pharmacologic studies have sought to design compounds of this class with minimal CNS toxicity.[4,7] We therefore synthesized a series of novel polar, water-soluble synthetic phenanthrene-based tylophorine derivatives (PBTs).[8] Because their increased polarity should prevent them from penetrating the blood−brain barrier, these compounds are likely to have little or no CNS toxicity.[3] One of these compounds, phenanthrene-based tylophorine derivative-1 (PBT-1), displayed potent cytotoxic activity against the human lung cancer cell line A549.[3] Its ability to inhibit the growth of human lung cancer cells is mediated through the downregulation of AKT phosphorylation and NF-κB signaling.[9] Since AKT and NF-κB signaling are known to play important roles in cancer metastasis and drug resistance[10,11] and the invasion and migration abilities of A549 cells have been shown to be suppressed by treatment with Akt inhibitor IV, dominant-negative AKT expression vector, or specific Akt siRNA,[12] this raises the possibility that PBT-1 may inhibit metastasis in lung cancer cells. An effective anticancer drug should selectively kill cancer cells while preventing metastasis. Although we previously demonstrated that PBT-1 displays selective cytotoxicity against lung adenocarcinoma cells,[9] it is not yet known whether PBT-1 inhibits lung adenocarcinoma cell metastasis. We therefore tested the ability of PBT-1 to inhibit metastasis in vitro and in vivo. We also sought to identify the direct targets of PBT-1 and their effects in inhibiting lung adenocarcinoma.

RESULTS

PBT-1 Reduces the Growth of Subcutaneous and Orthotopic Xenografts in Vivo. We previously showed that PBT-1 may have potential in the treatment of lung adenocarcinoma.[9,13] On the basis of its potent antiproliferative effects in vitro, we assessed the effects of PBT-1 on an in vivo CL1-5 tumor xenograft model. CL1-5 cells were subcutaneously injected into the flanks of nude mice. When the tumor size reached 100 mm^3 (generally after 5−8 days), the mice were intraperitoneally injected with PBT-1 (10 mg/kg per day) three times per week. In the absence of PBT-1, the tumors continued to grow, whereas PBT-1 treatment markedly inhibited tumor growth (Figure 1A). Interestingly, PBT-1 had little effect on body weight (Figure 1B) and had no overt toxicity under these experimental conditions. In addition, PBT-1 treatment inhibited the growth of orthotopic tumors induced by injection of CL1-5 cells into the thoracic cavity (Figure 1C) compared with control mice. Interestingly, PBT-1-treated mice developed fewer pulmonary nodules than vehicle (DMSO)-treated mice (Figure 1D).

PBT-1 Inhibits Migration and Invasion by Lung Adenocarcinoma Cells. We next examined the effects of PBT-1 on events associated with lung adenocarcinoma cell metastasis. Since PBT-1 can induce cell apoptosis and reduce cell viability at concentrations higher than 0.5 μg/mL,[9] its effects on lung adenocarcinoma cell migration and invasion were tested at concentrations of 0.1−0.75 μg/mL. The motility of CL1-5 cells treated with 0.25 μg/mL PBT-1 was significantly reduced compared with that of untreated CL1-5 cells in a wound-healing assay (Figure 2A). Similarly, invasion by CL1-5 cells, as determined by the Matrigel invasion assay, was dose-dependently reduced by PBT-1 (Figure 2B). Additionally, PBT-1-treated CL1-5 cells displayed reduced formation of filopodia (Figure 2C).

PBT-1 Represses Slug Expression and Upregulates E-Cadherin in Lung Adenocarcinoma Cells. Slug/E-cadherin signaling is critical in the cancer invasion and epithelial mesenchymal transition (EMT) pathways,[14,15] E-cadherin is a cell−cell adhesion molecule involved in epithelial adherent junctions. Slug is the EMT inducer responsible for transcriptional silencing of E-cadherin. High expression of Slug is associated with reduced E-cadherin expression and cancer metastasis.[16] Therefore, to investigate the mechanism by which PBT-1 inhibits lung adenocarcinoma cell metastasis, we examined its effects on Slug expression. Treatment of CL1-5 cells, which express high levels of Slug but low levels of E-cadherin (Figure 3A), with 0.5 μg/mL PBT-1 gradually reduced Slug expression, with no expression detected after 2 h (Figure 3B). Treatment of these cells with ≥0.5 μg/mL PBT-1, but not 0.25 μg/mL PBT-1, reduced Slug expression for up to 5 h (Figure 3C, upper panel). In contrast, PBT-1 dose-dependently increased the expression of E-cadherin in these cells (Figure 3C, upper panel), suggesting that the reduced expression of Slug is likely not due to reduced cell viability. To confirm that PBT-1 reduces Slug expression, we examined its effects on another primary lung adenocarcinoma cell line, CL152,[17] derived from a primary tumor with high Slug but low E-cadherin expression. Treatment of these cells with 0.5 μg/mL PBT-1 reduced Slug expression, whereas PBT-1 dose-dependently increased E-cadherin expression (Figure 3C, middle panel). Finally, since overexpression of Slug has been shown to confer EGFR-TKI resistance even in EGFR-activating mutant cells,[18] we examined whether PBT-1 suppresses Slug expression in EGFR-TKI-resistant lung adenocarcinoma cells. We found that 0.5 μg/mL PBT-1 inhibited Slug expression in the gefitinib-resistant lung adenocarcinoma cell line PC9/gef, which has a deletion in exon 19 of EGFR (Figure 3C, lower panel). Taken together, these findings indicate that PBT-1 reduces the level of Slug in lung adenocarcinoma cells.

Identification of Cellular PBT-1 Targets. To further explore the mechanism of action of PBT-1, we employed chemical proteomics to identify its cellular targets. In this approach, PBT-1 had to be modified such that the modified PBT-1 would not only retain its antitumor activity but also contain a reactive group that could couple to the matrix of Sepharose beads to pull down the potential interacting targets. We synthesized PBT-1-6L (Figure 4A, upper panel), an analogue of PBT-1 (Figure 4A, lower panel) for this particular study. The structure of PBT-1-6L contains two potential coupling functionalities (NH_2 and OH), one of which (NH_2) is used for conjugation to *N*-hydroxysuccinimide (NHS)-activated Sepharose 4B for affinity chromatography. PBT-1-6L coupled to Sepharose 4B is believed to retain its natural binding ability and can form tight association with the bound proteins. The IC_{50} of PBT-1-6L on CL1-5 is 0.5 μg/mL, which is comparable to that by PBT-1.[9] Incubation of CL1-5 cells with ≥0.5 μg/mL PBT-1-6L markedly reduced Slug expression, indicating that this PBT-1 derivative retains the antitumor activity of the parent compound (Figure 4B). To identify the putative proteins targeted by PBT-1, proteins from CL1-5 cell lysates were subjected to affinity chromatography using an NHS-activated Sepharose 4B matrix coupled with PBT-1-6L. Many proteins were detected in the fractions eluted from PBT-1-6L-coupled Sepharose 4B, whereas few or none were eluted from the bead

dx.doi.org/10.1021/jm401686b | J. Med. Chem. 2014, 57, 677−685

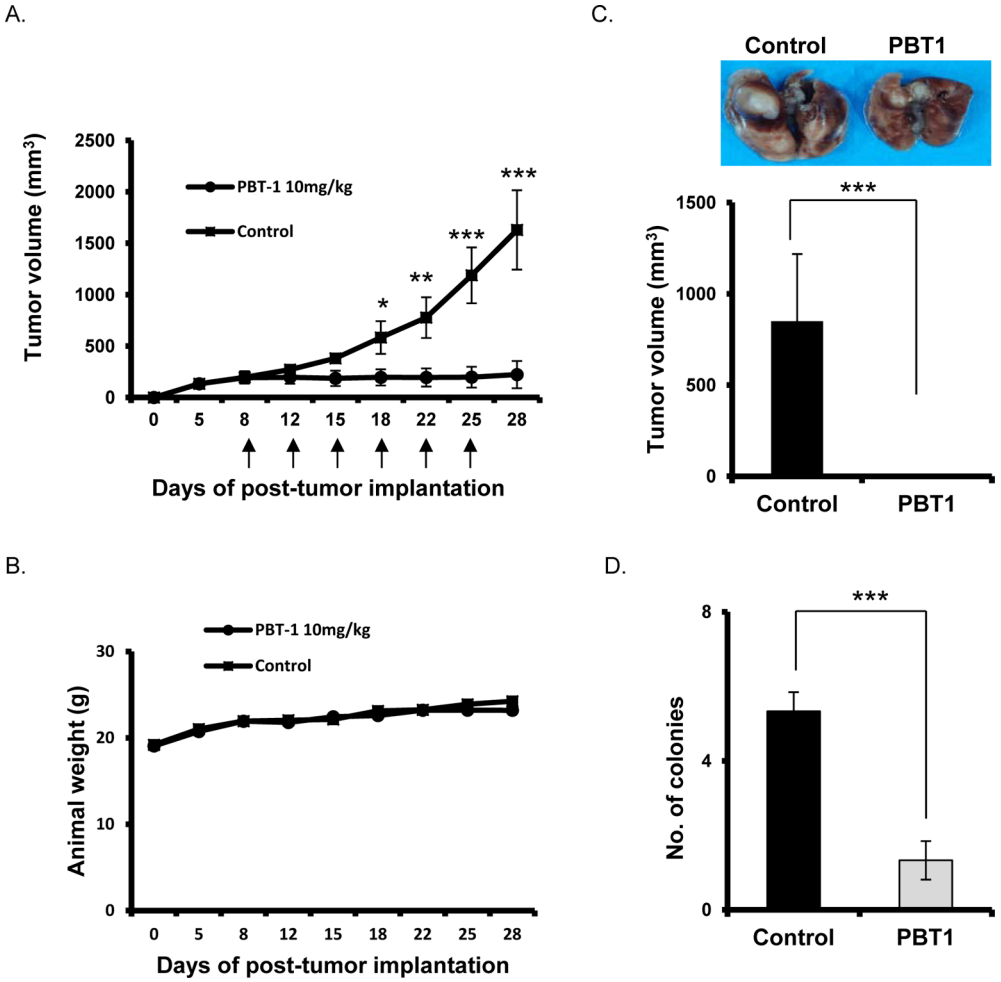

Figure 1. Effects of PBT-1 on the in vivo growth of lung adenocarcinoma subcutaneous and orthotopic xenografts. (A, B) Effects of PBT-1 on subcutaneous xenografts of lung adenocarcinoma cells. Lung adenocarcinoma CL1-5 cells were injected subcutaneously into the flank of each mouse; when tumor volumes reached 100 mm^3, the mice were intraperitoneally (i.p.) injected with PBT-1 (10 mg/kg per day) three times per week. Tumor volumes (A) and body weights (B) were determined twice weekly. (C, D) Effects of PBT-1 on orthotopic xenografts of lung adenocarcinoma cells. CL1-5 cells were orthotopically inoculated into the pleural cavities of nude mice ($n = 6$ per group). Five days later, mice were injected i.p. with PBT-1 three times per week, and tumor volumes in the excised lungs were measured 4 weeks later. Upper panel of (C): Representative lungs were excised from mice injected with CL1-5 cells treated with PBT-1 or vehicle (DMSO). Lower panel of (C): Quantitative evaluation of lung tumor volumes (mean ± SD, $n = 6$) in each group. (D) Number of metastatic tumor nodules in mice. Results shown are the means ± SD of six mice. *, $p < 0.05$; **, $p < 0.01$ by unpaired t-tests.

control (Figure 4C). The proteins eluted from PBT-1-6L-coupled Sepharose 4B were divided into 11 equal fractions, and following in-gel digestion with trypsin, they were further identified using an LTQ Orbitrap and Proteome Discoverer software. A total of 585 proteins were identified (Supplementary Table 1 in the Supporting Information); the 10 putative target proteins with the highest scores, as determined by Proteome Discoverer software, are listed in Table 1.

Previously, heat shock protein 90 (HSP90) and heterogeneous nuclear ribonucleoproteins A2/B1 (hnRNP A2/B1) were correlated to cellular survival in many cancers.[19,20] HSP90 is a highly conserved chaperone molecule that plays an important role in cellular homeostasis by modulating stabilization and activation of several proteins involved in a variety of cellular processes such as signal transduction, cell cycle regulation, and stress responses.[21] Many cochaperones assist HSP90 in its chaperone activity. In addition, hnRNP A2/B1 are members of the family of heterogeneous nuclear ribonucleoproteins A/B (hnRNP A/B), which are involved in cellular proliferation, differentiation, and protein synthesis in cancers.[22] We identified HSP90 and hnRNP A2/B1 as possible PBT-1-targeted proteins (Table 1). Many HSP90-associated cochaperones, such as HSP90-α, HSP gp96, HSP60, HSP71, HSP27, HSP10, and DNAJ cochaperones, were also identified in this study (marked in red in Supplementary Table 1 in the Supporting Information). This is thought to proceed by an interaction between PBT-1 and HSP90 and/or hnRNPA2/B1.

Lysates from CL1-5 cells were incubated in the presence or absence of free PBT-1-6L at 1 mM for 1 h and then fractionated on an NHS-activated Sepharose 4B matrix coupled with PBT-1-6L.[23] As shown in Figure 5A, in the absence of free PBT-1-6L competitor, HSP90 and hnRNP A2/B1 were detected in the fraction eluted from the PBT-1-6L-coupled Sepharose 4B matrix but not from the uncoupled beads. Upon preincubation of cell extract with an excess of free PBT-1-6L before fractionation, HSP90 and hnRNP A2/B1 were no longer detected in the fraction eluted from the PBT-1-6L-coupled Sepharose 4B matrix, indicating that the binding of HSP90 and hnRNP A2/B1 to PBT-1-6L is specific. To exclude the possibility that the observed binding may be attributed to the abundance of these two proteins

dx.doi.org/10.1021/jm401686b | J. Med. Chem. 2014, 57, 677−685

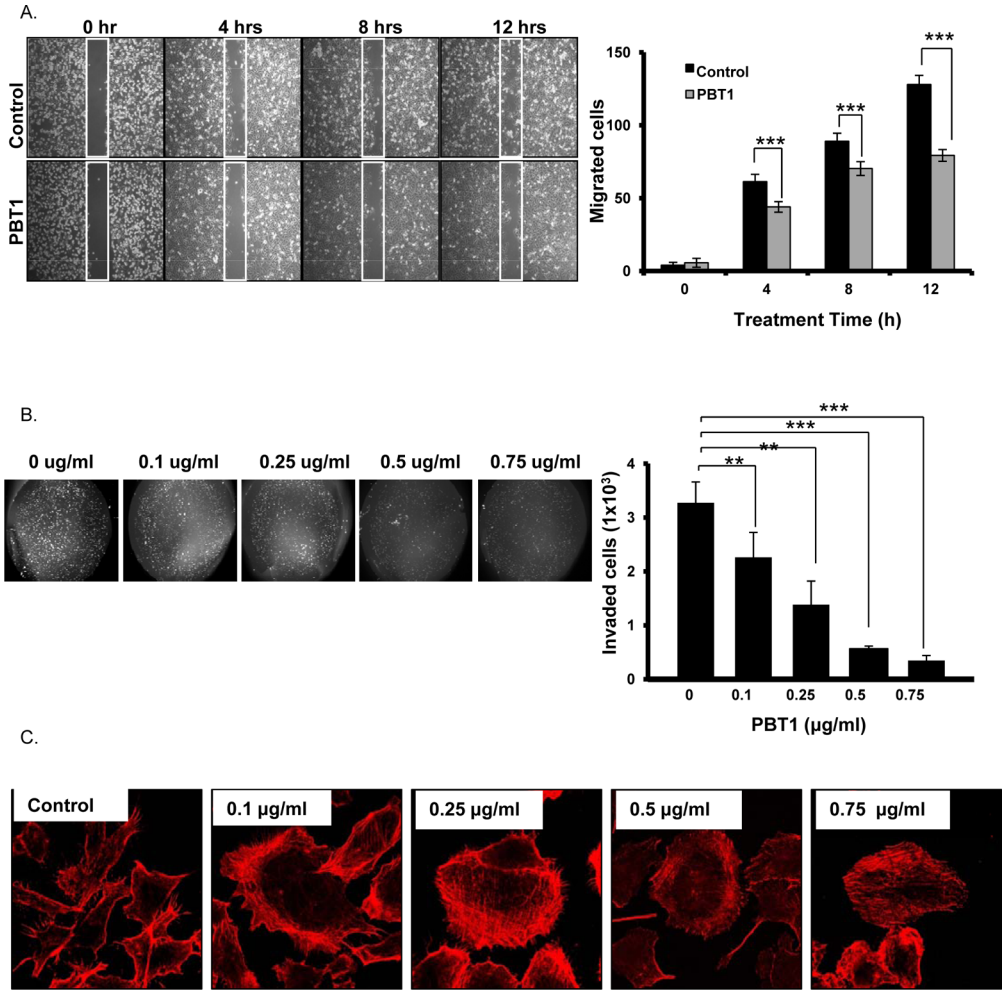

Figure 2. Effects of PBT-1 on cell motility, invasion, and filopodia formation by lung adenocarcinoma cells. CL1-5 cells were treated with PBT-1 and their (A) migration, (B) Matrigel invasion, and (C) formation of filopodia were assayed as described in Materials and Methods. The data shown are means ± SD from three independent experiments. **, $p < 0.01$; ***, $p < 0.001$ by unpaired *t*-tests.

in the cell lysate, we examined whether the other abundant proteins, β-actin and HSP70, could be detected in the fraction eluted from the PBT-1-6L-coupled Sepharose 4B matrix. As shown in Figure 5A, β-actin and HSP70 were not detected in the fraction eluted from the PBT-1-6L-coupled Sepharose 4B matrix, indicating that the detected binding of HSP90 and hnRNP A2/B1 to PBT-1 is not simply due to their abundance in the cells.

Inhibition of HSP90 and hnRNPA2 Reduces AKT and Slug Expression. To test whether PBT-1 regulates AKT and Slug expression by inhibiting HSP90, we assessed the effects of the HSP90 inhibitors geldanamycin (GA) and its derivative 17-allylamino-17-demethoxygeldanamycin (17-AAG)[19] on the levels of expression of AKT and Slug in CL1-5 cells. We found that treatment with GA and 17-AAG dose-dependently reduced the levels of phospho-AKT and Slug in CL1-5 cells (Figure 5B). However, the level of total AKT was reduced only after treatment with GA at high concentration (i.e., 2 μM). The decreased expression of Slug upon inhibition of HSP90 raises the possibility that Slug may be a client protein of HSP90. To test this postulate, we examined whether HSP90 and Slug could form a complex in CL1-5 cells. As shown in Figure 5C, HSP90 was readily detected in the immunoprecipitate pulled down by the anti-Slug antibody.

To assess whether PBT-1 interacts with and inhibits hnRNP A2/B1, we examined the effects of hnRNP A2/B1 depletion on the expression of AKT and Slug. Knockdown of hnRNP A2/B1 by two independent short hairpin RNA (shRNA) sequences (A2/B1#1 and A2/B1#2) greatly reduced the expression of hnRNP A2/B1 and Slug while increasing the expression of E-cadherin (Figure 5D). These cells also showed reduced activation of AKT, albeit to a lesser extent. Taken together, these results indicate that inhibition of the PBT-1 target proteins HSP90 and hnRNP A2/B1 can reduce Slug expression and AKT activation in lung adenocarcinoma cells (Figure 5E).

■ DISCUSSION

We previously reported that PBT-1 inhibits lung cancer cell growth in vitro through the Akt and NF-κB pathways.[9] Here we have shown that PBT-1 also inhibits metastatic activity, as evidenced by its inhibition of the migration, invasion, and filopodia formation of lung adenocarcinoma CL1-5 cells in vitro. Importantly, we also found that both the antitumor and anti-metastatic activities of PBT-1 function against CL1-5 xenografts in nude mice. These findings that PBT-1 selectively kills and inhibits the metastasis of lung adenocarcinoma suggest that this compound may have clinical applications.

In assessing the antimetastatic mechanism of action of PBT-1, we found that it inhibits the expression of Slug, a member of the Snail family of zinc finger transcription factors that regulate phenotypic changes in cancer cells. Slug is known to be a critical

dx.doi.org/10.1021/jm401686b | J. Med. Chem. 2014, 57, 677−685

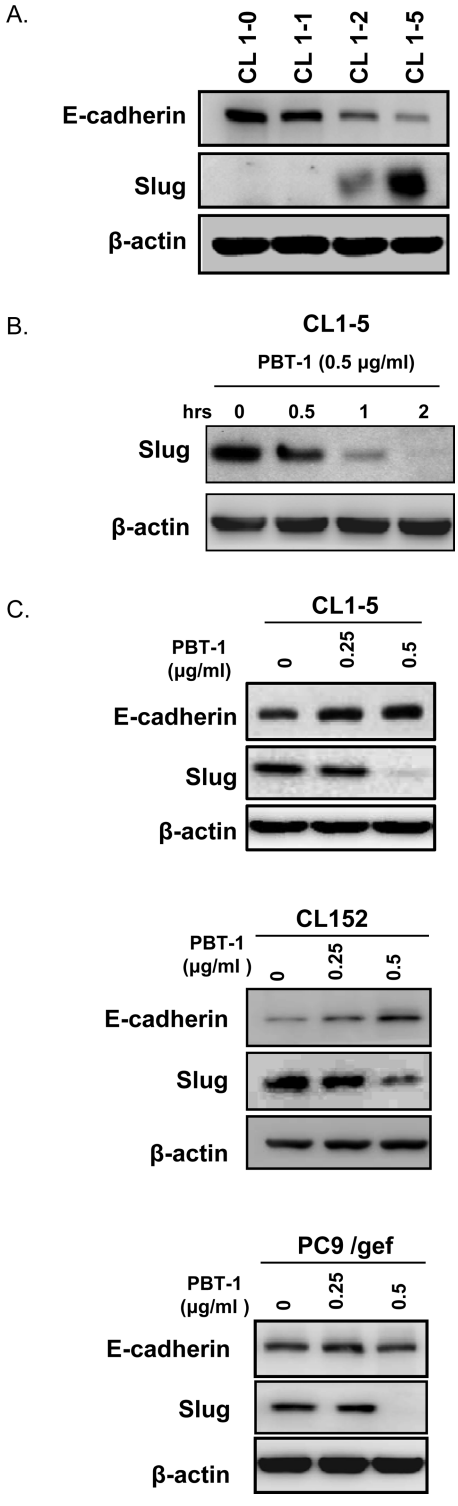

Figure 3. Effects of PBT-1 on the expression of Slug and E-cadherin. (A) Western blotting showing the levels of expression of Slug and E-cadherin in a panel of lung cancer cell lines with increasing invasion ability (CL1-0, CL1-1, CL1-2, and CL1-5). (B) Effects of PBT-1 on the kinetic expression of Slug and E-cadherin. CL1-5 cells were treated with 0.5 μg/mL PBT-1 and cultured for 0.5, 1, or 2 h, after which Slug expression in cell extracts was analyzed by Western blotting. (C) CL1-5 (upper panel), CL152 (middle panel), and PC9/gef (lower panel) cells were treated with various concentrations of PBT-1 and cultured for 5 h, after which Slug expression was analyzed by Western blotting. β-Actin served as the loading control. The results shown are representative of three similar experiments.

player in the cancer cell invasiveness and EMT pathways.[14,24] Overexpression of Slug was recently shown to confer EGFR-TKI resistance even on EGFR-activating mutant cells.[18] Knockdown of Slug expression has been reported to increase cellular sensitivity to chemotherapeutic drugs.[15] Therefore, inhibition of the Slug pathway may offer a novel path in the development of drugs against lung adenocarcinoma. Our finding that PBT-1 can inhibit the expression of Slug suggests that this compound may act as a Slug inhibitory modulator in cancer cells and may be used to treat patients with lung adenocarcinomas that display EGFR-TKI resistance. Indeed, we found that PBT-1 inhibited Slug expression in the gefitinib-resistant lung adenocarcinoma cell line PC9/gef.

Using a chemical proteomics approach, we attempted to identify the putative cellular targets of PBT-1. We identified 585 proteins that bound to and were eluted from PBT-1-6L-coupled Sepharose 4B, suggesting that these proteins are bound by PBT-1. HSP90 and hnRNP A2/B1 are two of the 10 putative target proteins with the highest scores as determined by Protein Discoverer software. Here we have presented evidence that the binding of PBT-1 to these two proteins is specific (Figure 5A). Also, although it is presently not known how PBT-1 binds to HSP90 and hnRNP A2/B1, we found that inhibition of HSP90 and hnRNP A2/B1 reduced Slug and phospho-AKT expression, suggesting that PBT-1 inhibition of Slug is due, at least in part, to inhibition of HSP90 and/or hnRNP A2/B1. Taken together, our data suggest that the binding of PBT-1 to HSP90 and hnRNP A2/B1 may inhibit Slug expression and AKT activation, accounting for the observed antitumor and antimetastatic activities of PBT-1. Therefore, PBT-1 is a novel inhibitory modulator of Slug expression that should be further explored for its potential clinical application against lung adenocarcinoma.

MATERIALS AND METHODS

Chemicals, Media, Antibodies, and Oligonucleotides. Culture media, chemical compounds, and fetal bovine serum (FBS) were purchased from Life Technologies (Grand Island, NY, USA). Antibodies against phospho-AKT (Ser473) and geldanamycin were purchased from Cell Signaling (Temecula, CA, USA); antibodies against AKT, Slug, and hnRNP A2/B1 were purchased from Santa Cruz Biotechnology (Santa Cruz, CA, USA); antibodies against HSP90 and HSP70 were purchased from Enzo Life Sciences (Farmingdale, NY, USA); and antibodies against E-cadherin and β-actin were purchased from BD Sciences (San Jose, CA, USA) and Sigma (St Louis, MO, USA), respectively. The HSP90 inhibitor 17AAG was purchased from Calbiochem (Gibbstown, NJ, USA). The phenanthrene-based derivatives PBT-1 and PBT-1-6L (see Figure 4A for their structures) were synthesized in the laboratory of Dr. K. H. Lee. NHS-activated Sepharose 4B was obtained from GE Healthcare (Piscataway, NJ, USA). All oligonucleotides were obtained from Bio Basic (Markham, ON, Canada).

Cell Lines and Cultivation of Cells. A panel of lung cancer cell lines with increasing invasion ability (CL1-0, CL1-1, CL1-2, and CL1-5) was established using a chamber selection system.[25] The human gefitinib-sensitive lung adenocarcinoma cancer cell line PC9, which contains a deletion in exon 19 of EGFR, and its gefitinib-resistant variant PC9/gef, which was selected by continuously exposing parental PC9 cells to increasing gefitinib concentrations for about 6 months, have been described previously.[18] The human lung cancer cell line CL152 was established in our laboratory from a patient with lung adenocarcinoma. All lung adenocarcinoma cells were cultivated in RPMI-1640 medium containing 10% FBS, 2 mM sodium pyruvate, 100 units/mL penicillin, and 100 units/mL streptomycin. The virus-packaging cell line 293T was cultured in DMEM containing 10% FBS. All cells were grown at 37 °C in a humidified incubator containing 5% CO_2.

dx.doi.org/10.1021/jm401686b | J. Med. Chem. 2014, 57, 677−685

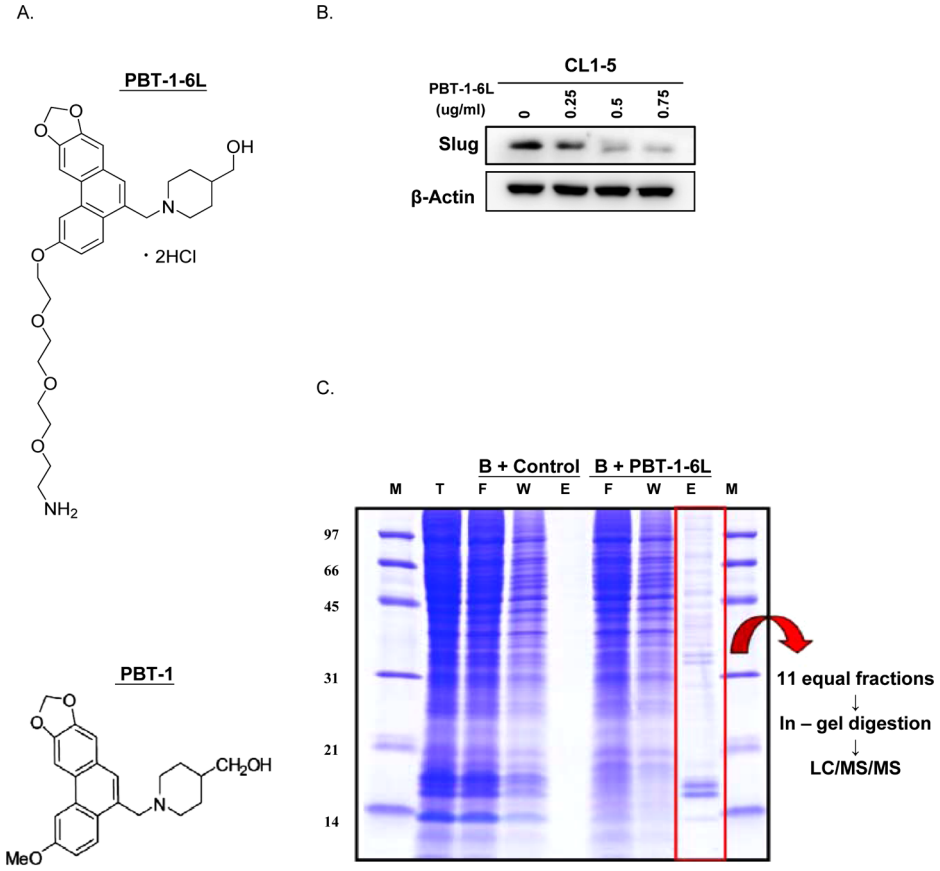

Figure 4. Identification of cellular PBT-1 targets. (A) Chemical structures of PBT-1-6L (upper panel) and PBT-1 (lower panel). (B) Effects of PBT-1-6L on Slug expression. CL1-5 cells were treated with various concentrations of PBT-1-6L for 24 h, and Slug expression was analyzed by Western blotting. β-Actin expression served as a loading control. (C) Affinity chromatography of the PBT-1 targeted proteins. Lysates from CL1-5 cells were fractionated on an NHS-activated Sepharose 4B matrix precoupled with PBT-1-6L. The proteins from the flow-through (F), the wash (W), and the elution (E) were resolved by 15% SDS-PAGE. The gel was divided into 11 equal slices, and the proteins in each slice were digested with trypsin and analyzed by LC/MS/MS. M, marker; B, NHS-activated Sepharose 4B beads.

Table 1. Identities of the 10 Highest-Scored Putative Proteins Targeted by PBT-1[a]

rank	identity	score
1	heat shock protein 90 kDa	1863.36
2	HIST1H2BM protein	1793.68
3	histone H2B.1	1589.82
4	heat shock protein 90 α isoform 2	1414.32
5	heat shock protein 60, mitochondria	1307.54
6	histone H1.2	1263.35
7	heterogeneous nuclear ribonucleoproteins A2/B1 isoform B1	1174.44
8	ATP-dependent RNA helicase A	1158.74
9	heterogeneous nuclear ribonucleoproteins Q1	1111.15
10	heterogeneous nuclear ribonucleoproteins M isoform B	1062.00

[a]Proteins were identified by Mascot (Matrix Science), and their classification, grouping, and FDR estimation were assessed using Protein Discoverer.

Cytotoxicity Assay. Cells (2×10^3/well) were plated in 24-well plates. After 24 h, the cells were treated with different concentrations of drug for 48 h. The treated cells were then fixed and stained with 0.5% methylene blue in 50% ethanol for 2 h. After the cells were washed with tap water to remove unbound stain, the plates were dried and then 1% sarkosyl was added to lyse the cells. Cell growth was quantified on the basis of the amount of methylene blue adsorbed to the cells as measured by a spectrophotometer (Molecular Devices) at 595 nm. IC_{50} was defined as the concentration of drug that inhibited cell growth by 50% after continuous drug exposure for 48 h.

Plasmids. Plasmids expressing shRNAs for knockdown of hnRNP A2/B1 were constructed by inserting the sequences 5′-GGAUUAUUUAAUAACAUUA-3′ (A2/B1#1) and 5′-GGAGAGUAGUUGAGCCAAA-3′ (A2/B1#2) into pSUPER retro.puro (pSR) vector (Oligoengine, Seattle, WA, USA) following the manufacturer's suggestions. The plasmid pSR-Luc was constructed by inserting into pSR the sequence 5′-CGTACGCGGAATACTTCGA-3′, which targets firefly luciferase mRNA.

Transfection, Preparation of Retrovirus Particles, and Infection. Plasmid DNAs were transfected into cells using Lipofectamine 2000 (Invitrogen, Carlsbad, CA, USA) according to the manufacturer's protocol. The retrovirus-packaging plasmid pCMVD8.2 (with Gag-Pol DNA) and the vesicular stomatitis virus envelope plasmid pMD.G were provided by the consortium (Academia Sinica, Taipei, Taiwan). Retroviral particles were generated by cotransfection of 293T cells with the retroviral plasmid and pVSV-G plasmid (BD Biosciences). After culturing at 37 °C for 18−20 h, the supernatant was removed and replaced with fresh medium. After incubation for another 48 h, medium containing viral particles was collected by centrifugation at 2000 rpm for 10 min at 4 °C. CL1-5 cells were infected with viral particles in the presence of Polybrene at 6 μg/mL. Stably infected CL1-5 cells were obtained by culturing the infected cells in the presence of 0.8 μg/mL puromycin for 2−3 weeks.

Immunoprecipitation and Western Blotting. Immunoprecipitation and Western blotting were performed as described previously.[26]

Invasion Assay. Transwell chambers (8 μm pore size; Falcon) were coated with 5 μg/mL Matrigel (Becton Dickinson Labware), and the top of each chamber was seeded with 2.5×10^4 cells in medium containing 10% NuSerum (Life Science). Following incubation for 20 h, the cells

dx.doi.org/10.1021/jm401686b | J. Med. Chem. 2014, 57, 677−685

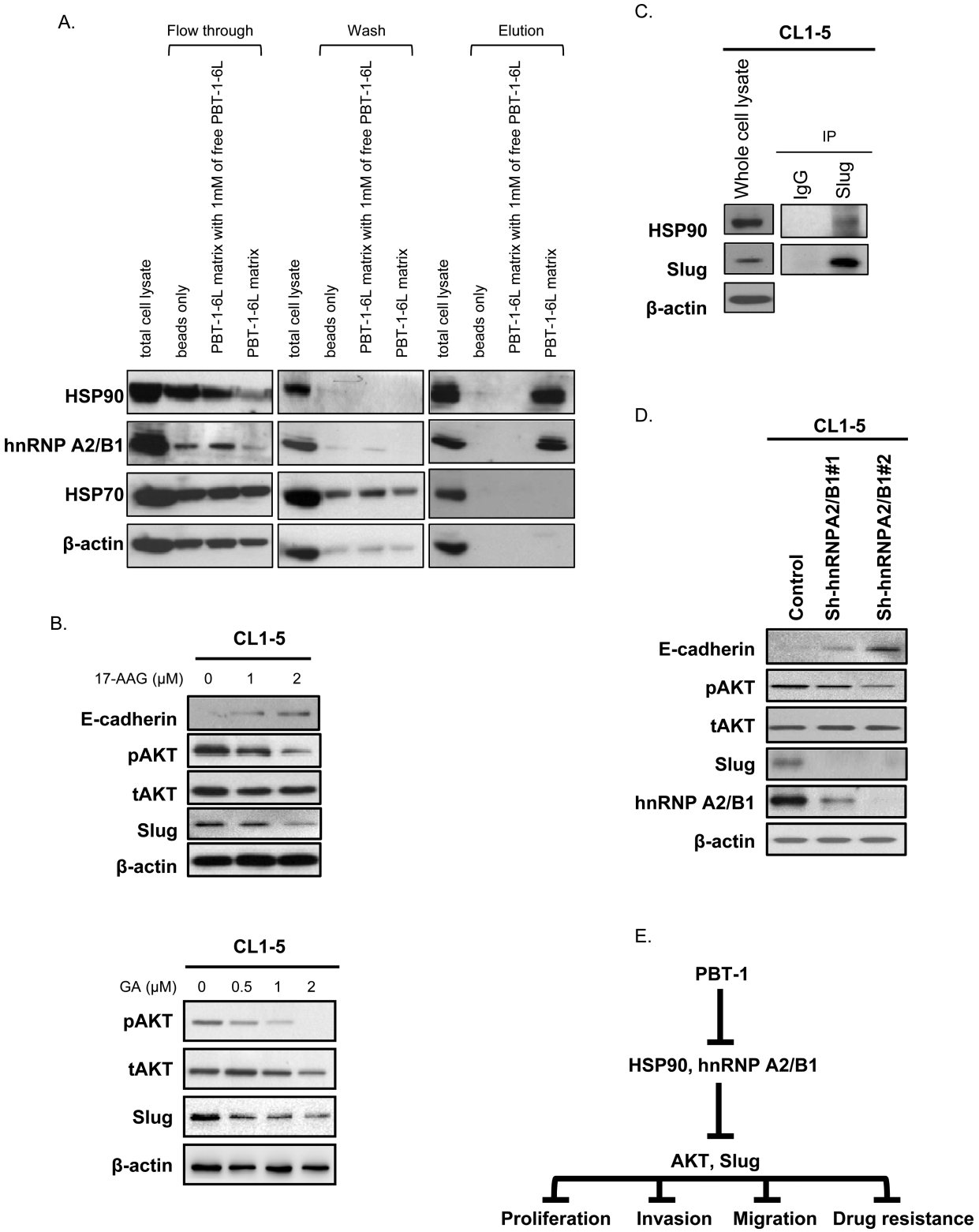

Figure 5. Effects of HSP90 and hnRNPA2 inhibition on AKT activation and Slug expression. (A) Lysates from CL1-5 cells were fractionated on an NHS-activated Sepharose 4B matrix (beads only) or incubated with or without 1 mM PBT-1-6L for 1 h before fractionation on an NHS-activated Sepharose 4B matrix coupled with PBT-1-6L (PBT-1-6L matrix). The proteins from the flow-through, the wash, and the elution were assayed the presence of HSP90, hnRNP A2/B1, HSP70, and β-Actin by Western blot. (B) CL1-5 cells were treated with various concentrations of GA or 17-AAG for 16 h, and the levels of expression of Slug, E-cadherin, total AKT (tAKT), and phosphorylated AKT (pAKT) were assessed by Western blotting. (C) Interaction of endogenous Slug and HSP90 in CL1-5 cells. The cell extracts were immunoprecipitated with anti-Slug-conjugated agarose beads. The proteins in the immunoprecipitates were analyzed by Western blotting. (D) CL1-5 cells were infected with retroviruses expressing shRNAs against hnRNP A2/B1 (sh-hnRNPA2/B1#1 and shRNPA2/B1#2) or pSR-Luc (Control), and the levels of expression of hnRNP A2/B1, Slug, E-cadherin, tAKT, and pAKT were assessed by Western blotting. β-Actin served as the loading control. (E) Model for the mechanism of action of PBT-1. The antitumor and antimetastasis activities of PBT-1 are thought to result from its interaction with and inhibition of two major target proteins, HSP90 and hnRNP A2/B1, resulting in reduced AKT activation and Slug expression.

dx.doi.org/10.1021/jm401686b | J. Med. Chem. 2014, 57, 677−685

invading the bottom of each chamber were fixed with methanol and stained with 50 μg/mL propidium iodide (Sigma). The propidium iodide-positive signal was analyzed by Analytical Imaging Station software (Imaging Research). Each sample was assayed in triplicate.

Wound Healing Assay. Cells were seeded into 6 cm culture dishes and grown to a near-confluent monolayer. A 10 μL pipet tip was used to scratch a line across the middle of each dish, and the cellular debris was removed by washing with PBS. The cultures were incubated at 37 °C and photographed at 0, 4, 8, and 12 h. The number of cells that migrated into the cell-free zone was scored and evaluated. Each sample was assayed in triplicate, and a minimum of three independent experiments were performed.

Filopodia Formation Assay. Filopodia formation was assayed as described previously.[27]

Affinity Chromatography. PBT-1-6L was covalently coupled to an NHS-activated Sepharose 4B matrix (GE Healthcare), and control beads were generated in 50% DMSO/0.05 mol/L Na_2CO_3 as described by the manufacturer.

Cell lysates were prepared from CL1-5 cells cultured in 10 cm dishes by disruption in lysis buffer (50 mM Tris, pH 8.0, 150 mM NaCl, 1 mM dithiothreitol, 0.01% Nonidet P-40, 100 mM PMSF, 1× protease inhibitor mixture). The lysates were centrifuged at 14000*g* for 30 min, and an aliquot of the supernatant containing 10 mg of protein was applied to each PBT-1-6L-coupled Sepharose 4B column (12 × 8 mm) at 4 °C. The mobile phase was washed with T buffer (50 mM Tris-HCl, pH 7.5, 1 mM PMSF, 100 mM NaCl, 10 mM 6-aminohexanoic acid, 1 mM benzamidine hydrochloride, 1 mM EDTA) at a flow rate of 500 μL/min. The bound proteins were eluted with T1 buffer (4 M urea, 1 M NaCl in T buffer) at a flow rate of 0.5 μL/min.

In-Gel Digestion, Mass Spectrometry Analysis, and Protein Identification. The proteins eluted from the affinity column were resolved by 15% SDS-PAGE and stained with Coomassie blue. The gel was cut into 11 equal slices, each of which was digested with trypsin, and the extracted peptides were subjected to LC/MS/MS analysis as described elsewhere.[28] The identities of these proteins were assessed using Mascot (www.matrixscience.com), and the protein inference, grouping, and false discovery rate (FDR) were estimated by Protein Discoverer. The algorithm in the Mascot search engine calculates the probability that the match of an investigational spectrum to a database is random using the equation S (ion score) = $-10 \log_{10}(P)$, where P is the absolute probability. Thus, a probability of 10^{-10} becomes a score of 100. These types of probabilistic scores are influenced by the search parameters and the size of the database. Thus, Mascot also calculates the threshold with a set value of $P = 0.05$; that is, a match is significant if it could be predicted to be random at a frequency of less than 5%. The protein score is the sum of the ion scores of all peptides; if a peptide has more than one spectral match, the highest-scoring match is used to calculate the final protein score.

Tumorigenesis in Animals. Six-week-old male BALB/c nu/nu mice maintained in a specific pathogen free (SPF) environment were inoculated subcutaneously in the right flank with 1×10^6 tumor cells in a volume of 100 μL on day 0. Treatment was initiated when the tumors were 100 mm^3 in volume. Six mice each were randomly treated with the compound being tested or vehicle, both injected i.p. three times per week. The tumor width (W) and length (L) were measured once weekly with calipers, and the tumor volume (V) was calculated according to the formula $V = 0.5W^2L$. All animal experiments were performed in accordance with the guidelines for the Animal Care Ethics Commission of our institution under an approved animal protocol.

In Vivo Metastasis Assay. CL-15 cells were injected into the pleural cavities of 6-week-old BALB/c nu/nu mice,[17] with six mice each treated with the compound or vehicle injected i.p. three times per week. Twenty-eight days after implantation, the mice were sacrificed by anesthesia with carbon dioxide, and all of the organs were removed and fixed in 10% formalin. The number of lung nodules was counted by gross and microscopic examination.

Statistical Analysis. Student's *t*-test was performed using the Statistical Package for the Social Sciences, version 12.0 (SPSS, Inc.). Differences between the variables were considered significant for p values less than 0.05.

■ ASSOCIATED CONTENT

Ⓢ Supporting Information

Identities of putative proteins targeted by PBT-1. This material is available free of charge via the Internet at http://pubs.acs.org.

■ AUTHOR INFORMATION

Corresponding Author

*Phone: 886-2-33662000. Fax: 886-2-23621877. E-mail: pcyang@ntu.edu.tw.

Author Contributions

[∞]C.-Y.C. and S.-C.Y. contributed equally.

Author Contributions

C.-Y.C., S.-C.Y., and P.-C.Y. conceived the experiments. C.-Y.C., S.-C.Y., K.-H.L., X.Y., T.-M.H., J.-C.L., and C.K. carried out the experiments. L.-P.C. and T.-C.V.W. collected and analyzed chemical proteomic and hnRNP A2/B1 data, respectively. C.-Y.C. and P.-C.Y. were the main writers of the manuscript. All of the authors were involved in writing the paper and gave final approval of the submitted and published versions.

Notes

The authors declare no competing financial interest.

■ ACKNOWLEDGMENTS

This study was supported by research grants from the National Science Council of the Republic of China (NSC101-2321-B-002-068, NSC102-2321-B-002-053, NSC98-2628-B-002-086-MY3, NSC100-2321-B-002-071, NSC 102-2320-B-255 -001, and NSC100-3112-B-006-005), National Taiwan University, Taipei, Taiwan (NTU10R71601-2, NTU101R7601-2, and NTU102R7601-2), Academia Sinica (520240129-3), Chang Gung Memorial Hospital (CMRPF1C0131), and Chang Gung University of Science and Technology (EZRPF3C0171, EZRPF3C0181, EZRPF3C0191, and EZRPF3C0201). This investigation was also supported by a grant from the National Cancer Institute, NIH, to K.-H.L. (CA177584).

■ ABBREVIATIONS USED

PBT-1, phenanthrene-based tylophorine derivative-1; PBT-1-6L, phenanthrene-based tylophorine derivative-1-6L; HSP90, heat shock protein 90; hnRNP A2/B1, heterogeneous nuclear ribonucleoproteins A2/B1.

■ REFERENCES

(1) Jemal, A.; Siegel, R.; Ward, E.; Hao, Y.; Xu, J.; Murray, T.; Thun, M. J. Cancer statistics, 2008. *CA-Cancer J. Clin.* **2008**, *58*, 71−96.

(2) Yang, P. Epidemiology of lung cancer prognosis: Quantity and quality of life. *Methods Mol. Biol.* **2009**, *471*, 469−86.

(3) Wei, L.; Shi, Q.; Bastow, K. F.; Brossi, A.; Morris-Natschke, S. L.; Nakagawa-Goto, K.; Wu, T. S.; Pan, S. L.; Teng, C. M.; Lee, K. H. Antitumor agents 253. Design, synthesis, and antitumor evaluation of novel 9-substituted phenanthrene-based tylophorine derivatives as potential anticancer agents. *J. Med. Chem.* **2007**, *50*, 3674−80.

(4) Gao, W.; Lam, W.; Zhong, S.; Kaczmarek, C.; Baker, D. C.; Cheng, Y. C. Novel mode of action of tylophorine analogs as antitumor compounds. *Cancer Res.* **2004**, *64*, 678−88.

(5) Komatsu, H.; Watanabe, M.; Ohyama, M.; Enya, T.; Koyama, K.; Kanazawa, T.; Kawahara, N.; Sugimura, T.; Wakabayashi, K. Phenanthroindolizidine alkaloids as cytotoxic substances in a Danaid butterfly, *Ideopsis similis*, against human cancer cells. *J. Med. Chem.* **2001**, *44*, 1833−6.

(6) Staerk, D.; Lykkeberg, A. K.; Christensen, J.; Budnik, B. A.; Abe, F.; Jaroszewski, J. W. In vitro cytotoxic activity of phenanthroindolizidine alkaloids from *Cynanchum vincetoxicum* and *Tylophora tanakae* against

drug-sensitive and multidrug-resistant cancer cells. *J. Nat. Prod.* **2002**, *65*, 1299−302.
(7) Shiah, H. S.; Gao, W.; Baker, D. C.; Cheng, Y. C. Inhibition of cell growth and nuclear factor-κB activity in pancreatic cancer cell lines by a tylophorine analogue, DCB-3503. *Mol. Cancer Ther.* **2006**, *5*, 2484−93.
(8) Wei, L.; Brossi, A.; Kendall, R.; Bastow, K. F.; Morris-Natschke, S. L.; Shi, Q.; Lee, K. H. Antitumor agents 251: Synthesis, cytotoxic evaluation, and structure−activity relationship studies of phenanthrene-based tylophorine derivatives (PBTs) as a new class of antitumor agents. *Bioorg. Med. Chem.* **2006**, *14*, 6560−9.
(9) Lin, J. C.; Yang, S. C.; Hong, T. M.; Yu, S. L.; Shi, Q.; Wei, L.; Chen, H. Y.; Yang, P. C.; Lee, K. H. Phenanthrene-based tylophorine-1 (PBT-1) inhibits lung cancer cell growth through the Akt and NF-κB pathways. *J. Med. Chem.* **2009**, *52*, 1903−11.
(10) Julien, S.; Puig, I.; Caretti, E.; Bonaventure, J.; Nelles, L.; van Roy, F.; Dargemont, C.; de Herreros, A. G.; Bellacosa, A.; Larue, L. Activation of NF-κB by Akt upregulates Snail expression and induces epithelium mesenchyme transition. *Oncogene* **2007**, *26*, 7445−56.
(11) Larue, L.; Bellacosa, A. Epithelial−mesenchymal transition in development and cancer: Role of phosphatidylinositol 3′ kinase/AKT pathways. *Oncogene* **2005**, *24*, 7443−54.
(12) Yu, Y. H.; Chen, H. A.; Chen, P. S.; Cheng, Y. J.; Hsu, W. H.; Chang, Y. W.; Chen, Y. H.; Jan, Y.; Hsiao, M.; Chang, T. Y.; Liu, Y. H.; Jeng, Y. M.; Wu, C. H.; Huang, M. T.; Su, Y. H.; Hung, M. C.; Chien, M. H.; Chen, C. Y.; Kuo, M. L.; Su, J. L. MiR-520h-mediated FOXC2 regulation is critical for inhibition of lung cancer progression by resveratrol. *Oncogene* **2013**, *32*, 431−43.
(13) Yang, X.; Shi, Q.; Liu, Y. N.; Zhao, G.; Bastow, K. F.; Lin, J. C.; Yang, S. C.; Yang, P. C.; Lee, K. H. Antitumor agents 268. Design, synthesis, and mechanistic studies of new 9-substituted phenanthrene-based tylophorine analogues as potent cytotoxic agents. *J. Med. Chem.* **2009**, *52*, 5262−8.
(14) Shih, J. Y.; Yang, P. C. The EMT regulator slug and lung carcinogenesis. *Carcinogenesis* **2011**, *32*, 1299−304.
(15) Shih, J. Y.; Tsai, M. F.; Chang, T. H.; Chang, Y. L.; Yuan, A.; Yu, C. J.; Lin, S. B.; Liou, G. Y.; Lee, M. L.; Chen, J. J.; Hong, T. M.; Yang, S. C.; Su, J. L.; Lee, Y. C.; Yang, P. C. Transcription repressor slug promotes carcinoma invasion and predicts outcome of patients with lung adenocarcinoma. *Clin. Cancer Res.* **2005**, *11*, 8070−8.
(16) Thiery, J. P. Epithelial−mesenchymal transitions in tumour progression. *Nat. Rev. Cancer* **2002**, *2*, 442−54.
(17) Chen, C. Y.; Jan, C. I.; Lo, J. F.; Yang, S. C.; Chang, Y. L.; Pan, S. H.; Wang, W. L.; Hong, T. M.; Yang, P. C. Tid1-L inhibits EGFR signaling in lung adenocarcinoma by enhancing EGFR ubiquitinylation and degradation. *Cancer Res.* **2013**, *73*, 4009−4019.
(18) Chang, T. H.; Tsai, M. F.; Su, K. Y.; Wu, S. G.; Huang, C. P.; Yu, S. L.; Yu, Y. L.; Lan, C. C.; Yang, C. H.; Lin, S. B.; Wu, C. P.; Shih, J. Y.; Yang, P. C. Slug confers resistance to the epidermal growth factor receptor tyrosine kinase inhibitor. *Am. J. Respir. Crit. Care Med.* **2010**, *183*, 1071−9.
(19) Trepel, J.; Mollapour, M.; Giaccone, G.; Neckers, L. Targeting the dynamic HSP90 complex in cancer. *Nat. Rev. Cancer* **2010**, *10*, 537−49.
(20) Tauler, J.; Zudaire, E.; Liu, H.; Shih, J.; Mulshine, J. L. hnRNP A2/B1 modulates epithelial−mesenchymal transition in lung cancer cell lines. *Cancer Res.* **2010**, *70*, 7137−47.
(21) Whitesell, L.; Lindquist, S. L. HSP90 and the chaperoning of cancer. *Nat. Rev. Cancer* **2005**, *5*, 761−72.
(22) Carpenter, B.; MacKay, C.; Alnabulsi, A.; MacKay, M.; Telfer, C.; Melvin, W. T.; Murray, G. I. The roles of heterogeneous nuclear ribonucleoproteins in tumour development and progression. *Biochim. Biophys. Acta* **2006**, *1765*, 85−100.
(23) Barrott, J. J.; Haystead, T. A. J. Hsp90, an unlikely ally in the war on cancer. *FEBS J.* **2013**, *280*, 1381−96.
(24) Nieto, M. A. The snail superfamily of zinc-finger transcription factors. *Nat. Rev. Mol. Cell Biol.* **2002**, *3*, 155−66.
(25) Chu, Y. W.; Yang, P. C.; Yang, S. C.; Shyu, Y. C.; Hendrix, M. J.; Wu, R.; Wu, C. W. Selection of invasive and metastatic subpopulations from a human lung adenocarcinoma cell line. *Am. J. Respir. Cell Mol. Biol.* **1997**, *17*, 353−60.
(26) Chen, C. Y.; Chiou, S. H.; Huang, C. Y.; Jan, C. I.; Lin, S. C.; Hu, W. Y.; Chou, S. H.; Liu, C. J.; Lo, J. F. Tid1 functions as a tumour suppressor in head and neck squamous cell carcinoma. *J. Pathol.* **2009**, *219*, 347−55.
(27) Pan, S. H.; Chao, Y. C.; Hung, P. F.; Chen, H. Y.; Yang, S. C.; Chang, Y. L.; Wu, C. T.; Chang, C. C.; Wang, W. L.; Chan, W. K.; Wu, Y. Y.; Che, T. F.; Wang, L. K.; Lin, C. Y.; Lee, Y. C.; Kuo, M. L.; Lee, C. H.; Chen, J. J.; Hong, T. M.; Yang, P. C. The ability of LCRMP-1 to promote cancer invasion by enhancing filopodia formation is antagonized by CRMP-1. *J. Clin. Invest.* **2011**, *121*, 3189−205.
(28) Chen, Y. J.; Lin, Y. P.; Chow, L. P.; Lee, T. C. Proteomic identification of Hsp70 as a new Plk1 substrate in arsenic trioxide-induced mitotically arrested cells. *Proteomics* **2011**, *11*, 4331−45.